AUTHOR QUERY FORM

	Journal: SAS	Please e-mail or fax your responses and any corrections to:
ELSEVIER	Article Number: 6839	E-mail: **corrections.essd@elsevier.sps.co.in** Fax: +31 2048 52799

Dear Author,

Any queries or remarks that have arisen during the processing of your manuscript are listed below and highlighted by flags in the proof. Please check your proof carefully and mark all corrections at the appropriate place in the proof (e.g., by using on-screen annotation in the PDF file) or compile them in a separate list.

For correction or revision of any artwork, please consult http://www.elsevier.com/artworkinstructions.

Articles in Special Issues: Please ensure that the words 'this issue' are added (in the list and text) to any references to other articles in this Special Issue.

Uncited references: References that occur in the reference list but not in the text – please position each reference in the text or delete it from the list.	
Missing references: References listed below were noted in the text but are missing from the reference list – please make the list complete or remove the references from the text.	

Location in article	Query / remark Please insert your reply or correction at the corresponding line in the proof
	No Queries

Electronic file usage
Sometimes we are unable to process the electronic file of your article and/or artwork. If this is the case, we have proceeded by:

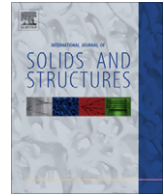☐ Scanning (parts of) your article   ☐ Rekeying (parts of) your article   ☐ Scanning the artwork

Thank you for your assistance.

Solutions of the interior and exterior boundary value problems in plane elasticity by using dislocation distribution layer

Y.Z. Chen *, X.Y. Lin

Division of Engineering Mechanics, Jiangsu University, Zhenjiang, Jiangsu 212013, People's Republic of China

ABSTRACT

Based on a previous publication (Savruk, 1981), a dislocation distribution layer method for the solution of interior and exterior boundary value problem (BVP) is studied in more detail. Properties of an integral operator in the resulting integral equation are studied. It is proved theoretically that the tractions applied on the outer boundary should be in equilibrium. In addition, a dislocation distribution layer method for the solution of exterior BVP is also suggested. In the exterior BVP, the tractions applied on the boundary may not be in equilibrium. In the exterior BVP, one must consider the single-valued condition of displacements. The formulation in the exterior BVP is not same as in the interior BVP. In the process of discretization, a technique for balance of the numbers of resulting algebraic equations and unknowns is suggested. Numerical examples prove that the suggested method can give sufficient accurate results.

© 2009 Published by Elsevier Ltd.

1. Introduction

The boundary integral equation (abbreviated as BIE) was widely used in elasticity, and the fundamental for BIE could be found from Rizzo (1967), Cruse (1969), Brebbia et al. (1984) and Jaswon and Symm (1997). The development of the boundary element method has been summarized recently (Cheng and Cheng, 2005). In the BIE, there are two kinds of formulation. One is the direct BIE method, and other is the indirect BIE method (Cheng and Cheng, 2005). In the direct BIE method, the unknown function is a function directly involved in the governing equation. However, in the indirect BIE method the unknown function is an intermediate function, which has a relation to the investigated function. Since both methods reflect the nature of the governing equation, for example, the Laplace equation, both methods can be used to solve boundary value problem (BVP). For the boundary value problem of the Laplace equation, the direct and indirect BIE methods were summarized (Cheng and Cheng, 2005).

In earlier years, some indirect BIE methods for plane elasticity were suggested (Muskhelishvili, 1953; Savruk, 1981). The BIE based on the dislocation distribution was studied by Savruk (1981), particularly, for the curved crack problem. A boundary integral equation with logarithmic kernel for the notch problem was formulated. In the formulation, the distributed dislocation density is taken to be the unknown function and the resultant force function to be the right hand term in the resulting integral equation (Chen and Cheung, 1994). A dislocation and point-force-based approach was suggested, which is used to formulate the boundary

element method (BEM) for plane elasticity in terms of Green's function that satisfy particular boundary conditions (Denda and Kosaka, 1997). Recently, a patch repair problem was solved. In the paper, one part of used complex potentials is based on the distributed dislocation layer in an infinite plate (Zemlyanova, 2007).

On the other hand, formulations of BIE may rely on the real or complex variables. In many cases, it is straightforward to formulate the BIE using the complex variable. The dual boundary element method in the real domain was extended to the complex variable dual boundary element domain (Chen and Chen, 2000). A review was given of complex variable based numerical solutions for Dirichlet potential problem in two and higher dimensions (Whitley and Hromadka, 2006).

Based on a previous publication (Muskhelishvili, 1953; Savruk, 1981), this paper studies formulation and numerical solutions of the interior and exterior boundary value problems in plane elasticity by using dislocation distribution layer. The dislocation distribution layer is assumed along a closed contour, and the complex potentials are defined on the whole complex plane. Behaviors of the defined complex potentials are studied in details.

A dislocation distribution layer method for the solution of interior BVP is suggested. Properties of an integral operator in the resulting integral equation are studied. It is proved theoretically that the tractions applied on the outer boundary must be in equilibrium. A discretization scheme is suggested to convert the integral equation into an algebraic equation. Properties of the influence matrix are discussed. Numerical examples prove that the suggested method can give sufficient accurate results.

In addition, a dislocation distribution layer method for the solution of exterior BVP is studied. In the exterior BVP, the

* Corresponding author. Tel.: +86 0511 88780780; fax: +86 0511 88791739.
E-mail address: chens@ujs.edu.cn (Y.Z. Chen).

tractions applied on the boundary may not be in equilibrium. When a moving point "z" moves in the exterior region, and a loop for the logarithmic function will be encountered. In this case, one must consider the single-valued condition of displacements. The formulation in the exterior BVP is not same as in the interior BVP. In the process of discretization, a technique for balance of the numbers of resulting algebraic equations and unknowns is suggested. Numerical examples prove that the suggested method can give sufficient accurate results.

2. General behaviors of complex potentials formulated on the dislocation distribution layer in an infinite plate

The complex variable function method plays an important role in plane elasticity. Fundamental of this method is introduced. In the method, the stresses $(\sigma_x, \sigma_y, \sigma_{xy})$, the resultant forces (X, Y) and the displacements (u, v) are expressed in terms of complex potentials $\phi(z)$ and $\psi(z)$ such that (Muskhelishvili, 1953)

$$\sigma_x + \sigma_y = 4\mathrm{Re}\,\Phi(z),$$
$$\sigma_y - \sigma_x + 2i\sigma_{xy} = 2[\bar{z}\Phi'(z) + \Psi(z)] \tag{1}$$

$$f = -Y + iX = \phi(z) + z\overline{\phi'(z)} + \overline{\psi(z)} \tag{2}$$

$$2G(u + iv) = \kappa\phi(z) - z\overline{\phi'(z)} - \overline{\psi(z)} \tag{3}$$

where $\Phi(z) = \phi'(z)$, $\Psi(z) = \psi'(z)$, a bar over a function denotes the conjugated value for the function, G is the shear modulus of elasticity, $\kappa = (3 - v)/(1 + v)$ in the plane stress problem, $\kappa = 3 - 4v$ in the plane strain problem, and v is the Poisson's ratio.

Except for the physical quantities mentioned above, from Eqs. (2) and (3) two derivatives in specified direction (abbreviated as DISD) are introduced as follows (Savruk, 1981; Chen and Lin, 2006; Chen, 2007):

$$J_1(z) = \frac{d}{dz}\{-Y + iX\} = \Phi(z) + \overline{\Phi(z)} + \frac{d\bar{z}}{dz}\left(\overline{z\Phi'(z)} + \overline{\Psi(z)}\right)$$
$$= \sigma_N + i\sigma_{NT} \tag{4}$$

$$J_2(z) = 2G\frac{d}{dz}\{u + iv\} = \kappa\Phi(z) - \overline{\Phi(z)} - \frac{d\bar{z}}{dz}\left(\overline{z\Phi'(z)} + \overline{\Psi(z)}\right)$$
$$= (\kappa + 1)\Phi(z) - J_1 \tag{5}$$

It is easy to verify that $J_1 = \sigma_N + i\sigma_{NT}$ denotes the normal and shear tractions along the segment $\overline{z, z + dz}$ (Fig. 1(a)). Secondly, the J_1 and J_2 values depend not only on the position of a point "z", but also on the direction of the segment "dz/dz".

In addition, the moment caused by the tractions applied along a curve "AB" can be evaluated by Muskhelishvili (1953)

$$M = \mathrm{Re}[\chi(z) - z\psi(z) - z\bar{z}\phi'(z)]\big|_A^B, \quad \text{where } \chi(z) = \int \psi(z)\,dz \tag{6}$$

Particularly, if the complex potentials $\phi(z)$ and $\psi(z)$ take the following expression:

$$\phi(z) = A_2 \ln z + a_0 + \sum_{k=1}^{\infty}\frac{a_k}{z^k}, \quad \psi(z) = B_2 \ln z + b_0 + \sum_{k=1}^{\infty}\frac{b_k}{z^k} \tag{7}$$

where A_2, a_o, B_2, b_o and a_k, b_k $(k = 1, 2, \ldots)$ are some constants. The moment caused by tractions applied on a sufficient large circle "CR" will be

$$M_{CR} = -2\pi\mathrm{Im}\,b_1 \tag{8}$$

In plane elasticity we generally meet the function in the form $f(z)\overline{g(z)}$, where $f(z)$ and $g(z)$ are two analytic functions, and the bar denotes the conjugate to the relevant argument. A particular derivative for the function $f(z)\overline{g(z)}$ is defined as

$$\frac{d}{dz}\left\{f(z)\overline{g(z)}\right\} = = f'(z)\overline{g(z)} + f(z)\overline{g'(z)}\frac{d\bar{z}}{dz} \tag{9}$$

which is called the derivative of the function $f(z)\overline{g(z)}$ in a specified direction (abbreviated as DISD) (Savruk, 1981; Chen and Lin, 2006; Chen, 2007). To distinguish the DISD, the symbol {} is always used for this kind of derivative. Particular feature of the DISD is that the result of DISD depends not only on the argument "z" (the position of a point in the complex plane) but also on the "$d\bar{z}/dz$" (the direction of a segment). The concept of DISD is important in the plane elasticity problem. In fact, the J_1 and J_2 shown by Eqs. (4) and (5) are DISD.

In plane elasticity, the following integrals are useful (Muskhelishvili, 1953; Savruk, 1981; Chen and Lin, 2006; Chen, 2007):

$$F(z) = \frac{1}{2\pi i}\int_L \frac{f(t)\,dt}{t - z} \tag{10}$$

$$G(z) = \frac{1}{2\pi i}\int_L \frac{g(t)\,d\bar{t}}{t - z} \tag{11}$$

$$H(z, \bar{z}) = \frac{1}{2\pi i}\int_L \frac{\bar{t} - \bar{z}}{(t - z)^2}h(t)\,dt \tag{12}$$

where L is a smooth curve or a closed contour. Also, we assume that the function $f(t)$, $g(t)$ and $h(t)$ satisfy the Hölder condition (Muskhelishvili, 1953). Sometimes, the functions $f(t)$, $g(t)$ and $h(t)$ are called the density functions hereafter. Clearly, the two integrals defined by Eqs. (10) and (11) are analytic functions, and one defined by Eq. (12) is not. The integral (10) is precisely the well-known Cauchy integral.

Generally speaking, these integrals take different values when $z \to t_0^+$ and $z \to t_0^-$, ($t_0 \in L$, or $t_0 \in \Gamma$ in Fig. 1(b)), respectively. The limit values of these functions from the upper and lower sides of the curve L are found to be (Muskhelishvili, 1953; Savruk, 1981; Chen and Lin, 2006; Chen, 2007)

$$F^{\pm}(t_o) = \pm\frac{f(t_o)}{2} + \frac{1}{2\pi i}\int_L \frac{f(t)\,dt}{t - t_o} \tag{13}$$

$$G^{\pm}(t_o) = \pm\frac{g(t_o)}{2}\frac{d\bar{t}_o}{dt_o} + \frac{1}{2\pi i}\int_L \frac{g(t)\,d\bar{t}}{t - t_o} \tag{14}$$

$$H^{\pm}(t_o, \bar{t}_o) = \pm\frac{h(t_o)}{2}\frac{d\bar{t}_o}{dt_o} + \frac{1}{2\pi i}\int_L \frac{\bar{t} - \bar{t}_o}{(t - t_o)^2}h(t)\,dt \tag{15}$$

In Eqs. (13)–(15), all the integrals should be understood in the sense of principal value of the integral. Note that, the notations of $f(t)$, $g(t)$, $h(t)$, $F(z)$, $G(z)$ and $H(z, \bar{z})$ used in Eqs. (10)–(15) have no relation with those mentioned in other places.

If a point dislocation is placed at the point $z = t$ as shown in Fig. 1(a), the corresponding potentials take the form (Savruk, 1981; Chen and Lin, 2006; Chen, 2007)

$$\phi(z) = H\log(z - t), \quad \Phi(z) = \phi'(z) = \frac{H}{z - t},$$
$$\Phi'(z) = -\frac{H}{(z - t)^2} \tag{16}$$

$$\psi(z) = \overline{H}\log(z - t) - \frac{H\bar{t}}{z - t}, \quad \Psi(z) = \psi'(z) = \frac{\overline{H}}{z - t} + \frac{H\bar{t}}{(z - t)^2} \tag{17}$$

where $H = H_1 + iH_2$ denotes the point dislocation applied at the point $z = t$ (Fig. 1(a)).

In Eqs. (16) and (17), if H is replaced by $-g'(t)\,dt/2\pi$ and one performs integration, the complex potentials caused by a dislocation distribution $g'(t)$ along the contour Γ are introduced (Fig. 1(b)) (Savruk, 1981; Chen and Lin, 2006; Chen, 2007)
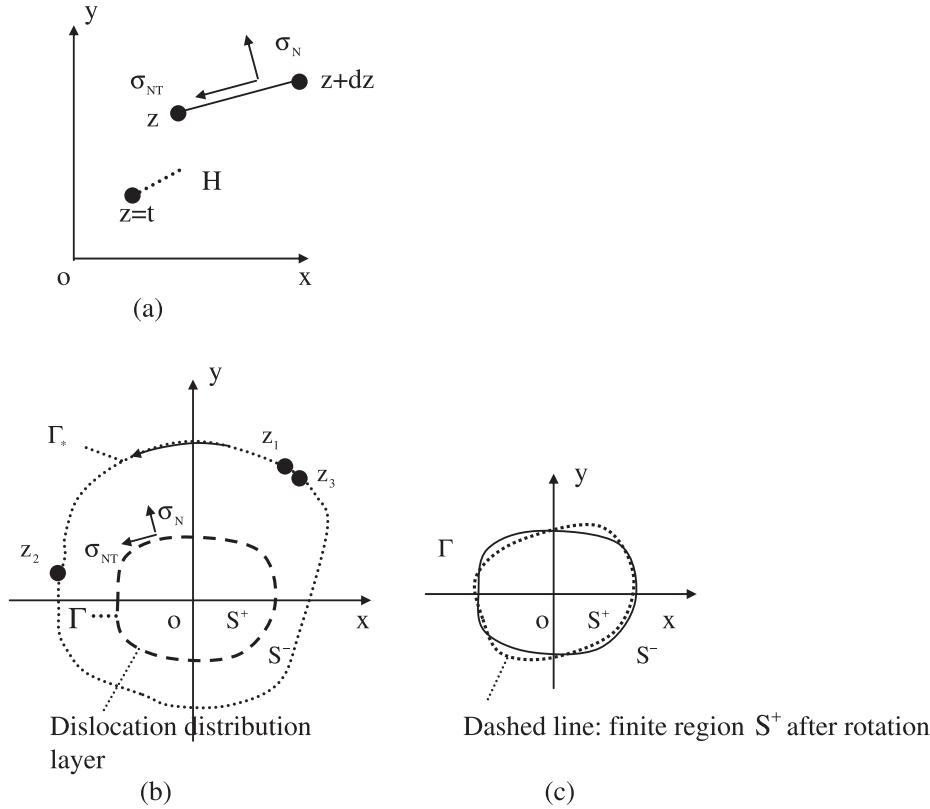
Fig. 1. (a) A concentrated dislocation with the intensity H at the point $z = t$. (b) Dislocation distribution layer along the closed curve Γ. (c) The non-stressed finite region S^+ after rotation, marked with the dash line.

$$\phi(z) = -\frac{1}{2\pi}\int_\Gamma \ln(z-t)g'(t)\,dt, \quad \phi'(z) = \frac{1}{2\pi}\int_\Gamma \frac{g'(t)\,dt}{t-z},$$

$$\phi''(z) = \frac{1}{2\pi}\int_\Gamma \frac{g'(t)\,dt}{(t-z)^2} \tag{18}$$

$$\psi(z) = -\frac{1}{2\pi}\int_\Gamma \ln(z-t)\overline{g'(t)}\,d\bar t - \frac{1}{2\pi}\int_\Gamma \frac{\bar t g'(t)\,dt}{t-z},$$

$$\psi'(z) = \frac{1}{2\pi}\int_\Gamma \frac{\overline{g'(t)}\,d\bar t}{t-z} - \frac{1}{2\pi}\int_\Gamma \frac{\bar t g'(t)\,dt}{(t-z)^2} \tag{19}$$

The complex potentials $\phi(z)$ and $\psi(z)$ may be defined in the interior region $z \in S^+$ or in the exterior region $z \in S^-$ (Fig. 1(b)).

After taking the following steps: (a) substituting Eqs. (18) and (19) into Eq. (4), (b) letting $z \to t_o^+$ or $z \to t_o^-$, and (c) using Eqs. (13)–(15), in both cases ($z \to t_o^+$ or $z \to t_o^-$) we will find (Fig. 1(b))

$$(\sigma_N(t_o) + i\sigma_{NT}(t_o))^+ = (\sigma_N(t_o) + i\sigma_{NT}(t_o))^-$$
$$= \frac{1}{\pi}\int_\Gamma \frac{g'(t)\,dt}{t-t_o} + \frac{1}{2\pi}\int_\Gamma K_1(t,t_o)g'(t)\,dt$$
$$+ \frac{1}{2\pi}\int_\Gamma K_2(t,t_o)\overline{g'(t)}\,d\bar t, (t_o \in \Gamma) \tag{20}$$

where

$$K_1(t,t_o) = \frac{d}{dt_o}\left\{\ln\frac{t-t_o}{\bar t-\bar t_o}\right\} = -\frac{1}{t-t_o} + \frac{1}{\bar t-\bar t_o}\frac{d\bar t_o}{dt_o}$$
$$K_2(t,t_o) = -\frac{d}{dt_o}\left\{\frac{t-t_o}{\bar t-\bar t_o}\right\} = \frac{1}{\bar t-\bar t_o} - \frac{t-t_o}{(\bar t-\bar t_o)^2}\frac{d\bar t_o}{dt_o} \tag{21}$$

Eq. (20) reveals that the traction component $(\sigma_N(t_o) + i\sigma_{NT}(t_o))$ is continuous when a point is moving across the boundary $t_o \in \Gamma$ (Fig. 1(b)).

In addition, after taking the following steps: (a) substituting Eqs. (18) and (19) into Eq. (5), (b) letting $z \to t_o^+$ or $z \to t_o^-$, and (c) using Eqs. (13)–(15), we will find

$$g'(t) = -\frac{2Gi}{\kappa+1}\frac{d[(u+iv)^+ - (u+iv)^-]}{dt}, \quad (t \in \Gamma) \tag{22}$$

Eq. (22) reveals that the displacement $(u + iv)$ is discontinuous when a point is moving across the boundary $t \in \Gamma$.

In the first case for $z \in S^+$ (Fig. 1(b)), the complex potentials $\phi(z)$ and $\psi(z)$ shown by Eqs. (18) and (19) represent a single-valued analytic function. In this case, the interior region is applied by the boundary tractions in equilibrium and the single-valued condition of displacements is satisfied automatically.

A particular case is interesting. Substituting $g'(t) = 1$ into Eqs. (18) and (19) yields

$$\phi'(z) = \frac{1}{2\pi}\int_\Gamma \frac{dt}{t-z} = i,$$
$$\psi'(z) = \frac{1}{2\pi}\int_\Gamma \frac{d\bar t}{t-z} - \frac{1}{2\pi}\int_\Gamma \frac{\bar t\,dt}{(t-z)^2} = 0, \quad (z \in S^+) \tag{23}$$

In the second case for $z \in S^-$ (Fig. 1(b)), the complex potentials $\phi(z)$ and $\psi(z)$ are not a single-valued analytic function in the region $z \in S^-$.

The contour increment for some functions plays an important role in the following analysis. When a point "z" is going around a large circle, or along the closed curve $z_1z_2z_3$ (or Γ_*) in Fig. 1(b) in anti-clockwise direction, the increment of a function saying for $\phi(z)$, is denoted as $\{\phi(z)\}_{in}$. From this definition and Eqs. (18) and (19), we have

$$\{\ln z\}_{in} = 2\pi i, \quad \{\phi(z)\}_{in} = -i\int_\Gamma g'(t)\,dt, \quad \{\phi'(z)\}_{in} = 0,$$

$$\{\psi(z)\}_{in} = -i\int_\Gamma \overline{g'(t)}\,d\bar{t} \tag{24}$$

In addition, using Eqs. (2) and (3) yields

$$\{f\}_{in} = \{-Y + iX\}_{in} = 0 \tag{25}$$

$$\{2G(u+iv)\}_{in} = -i(\kappa+1)\int_\Gamma g'(t)\,dt \tag{26}$$

By using Eqs. (7) and (19), we find that $b_1 = \frac{1}{2\pi}\int_\Gamma(t\overline{g'(t)}\,d\bar{t} + \bar{t}g'(t)\,dt)$ and b_1 takes a real value. Thus, from Eq. (8) we have

$$M_{CR} = -2\pi\,\mathrm{Im}\,b_1 = 0 \tag{27}$$

Eqs. (25) and (27) reveal that the tractions applied along the contour Γ_*, or along the closed curve $z_1 z_2 z_3$, are in equilibrium (Fig. 1(b)). However, from Eq. (26) we see that the displacements in the exterior region may not satisfy the single-valued condition.

A particular case is interesting. Substituting $g'(t) = 1$ into Eqs. (18) and (19) yields

$$\phi'(z) = \frac{1}{2\pi}\int_\Gamma \frac{dt}{t-z} = 0 \tag{}$$

$$\psi'(z) = \frac{1}{2\pi}\int_\Gamma \frac{d\bar{t}}{t-z} - \frac{1}{2\pi}\int_\Gamma \frac{\bar{t}\,dt}{(t-z)^2} = \frac{1}{2\pi}\int_\Gamma d\left(\frac{\bar{t}}{t-z}\right) = 0, \quad (z \in S^-) \tag{28}$$

From Eqs. (1), (23) and (28) we see that, $\sigma_{ij} = 0$ for $z \in S^+$ and $z \in S^-$ in the case of $g'(t) = 1$. This situation is easy to get explanation. It is assumed that the infinite plate has not been stressed (Fig. 1(c)). One can cut a finite portion from the infinite plate. In addition, let the finite portion have a small rotation γ, and the notched infinite plate preserves in a fixed position (Fig. 1(c)). In this case, we have

$$u + iv = i\gamma z, \quad (z \in S^+) \tag{29}$$

$$u + iv = 0, \quad (z \in S^-) \tag{30}$$

Therefore, the dislocation distribution along the contour Γ can be evaluated by

$$g'(t) = -\frac{2Gi}{\kappa+1}\frac{d[(u+iv)^+ - (u+iv)^-]}{dt} = \frac{2G\gamma}{\kappa+1} \tag{31}$$

If one lets $\gamma = (\kappa+1)/2G$, $g'(t) = 1$ is obtained.

3. Dislocation distribution layer method for the solution of interior boundary value problem (BVP)

3.1. Formulation of the integral equation for interior BVP

In the interior BVP, from Eq. (4) the boundary condition may be written as (Fig. 2)

$$J_1(t_o) = \sigma_N(t_o) + i\sigma_{NT}(t_o) = \tilde{\sigma}_N(t_o) + i\tilde{\sigma}_{NT}(t_o), \quad (t_o \in \Gamma) \tag{32}$$

where the boundary traction $\tilde{\sigma}_N(t_o) + i\tilde{\sigma}_{NT}(t_o)$ is given beforehand, which must be in equilibrium in general.

From Eq. (20), we will obtain the following integral equation:

$$\Lambda(t_o, g'(t); t \to t_o) = \tilde{\sigma}_N(t_o) + i\tilde{\sigma}_{NT}(t_o) \tag{33}$$

where

$$\Lambda(t_o, g'(t); t \to t_o) = \frac{1}{\pi}\int_\Gamma \frac{g'(t)\,dt}{t-t_o} + \frac{1}{2\pi}\int_\Gamma K_1(t,t_o)g'(t)\,dt + \frac{1}{2\pi}\int_\Gamma K_2(t,t_o)\overline{g'(t)}\,d\bar{t},$$

$$(\Lambda(t_o, g'(t); t \to t_o) \text{ abbreviated as } \Lambda(t_o) \text{ for } t_o \in \Gamma) \tag{34}$$

where the two integral kernels $K_1(t,t_o)$ and $K_2(t,t_o)$ have been defined by Eq. (21) previously. For the sake of compactness, the integral operator $\Lambda(t_o, g'(t); t \to t_o)$ is written as $\Lambda(t_o)$. The integral equation shown by Eq. (33) was obtained previously, particularly, for the curved crack problem (Savruk, 1981).

3.2. Properties of the integral operator $\Lambda(t_o)$

Several properties of the integral operator $\Lambda(t_o)$ are introduced below. The first property of the integral operator $\Lambda(t_o)$ is introduced as follows:

$$\Lambda(t_o)|_{g'(t)=1} = 0, \quad (t_o \in \Gamma) \tag{35}$$

Clearly, in the case of $g'(t) = 1$, $\Lambda(t_o)$ can be rewritten as

$$\Lambda(t_o)|_{g'(t)=1} = \frac{1}{2\pi}\left(M_1(t_o) + \frac{d\bar{t}_o}{dt_o}(M_2(t_o) + M_3(t_o))\right), \quad (t_o \in \Gamma) \tag{36}$$

where

$$M_1(t_o) = \int_\Gamma \frac{dt}{t-t_o} + \int_\Gamma \frac{1}{\bar{t}-\bar{t}_o}\,d\bar{t}, \quad (t_o \in \Gamma) \tag{37}$$

$$M_2(t) = \int_\Gamma \frac{1}{\bar{t}-\bar{t}_o}\,dt, \qquad M_3(t_o) = -\int_\Gamma \frac{t-t_o}{(\bar{t}-\bar{t}_o)^2}\,d\bar{t}, \quad (t_o \in \Gamma) \tag{38}$$

Since $\int_\Gamma \frac{dt}{t-t_o} = \pi i$, we have $M_1(t_o) = 0$. In addition, we have the following equality:

$$M_3(t_o) = -\int_\Gamma \frac{t-t_o}{(\bar{t}-\bar{t}_o)^2}\,d\bar{t} = \int_\Gamma d\left(\frac{t-t_o}{\bar{t}-\bar{t}_o}\right) - \int_\Gamma \frac{dt}{\bar{t}-\bar{t}_o} = -M_2(t_o) \tag{39}$$

Finally, from Eqs. (36)–(39), the property $\Lambda(t_o)|_{g'(t)=1} = 0$ shown by Eq. (35) is proved.

Eq. (35) reveals that the homogenous integral equation $\Lambda(t_o) = 0$ may have a non-trivial solution $g'(t) = 1$. Alternatively speaking, the integral equation $\Lambda(t_o) = \tilde{\sigma}_N(t_o) + i\tilde{\sigma}_{NT}(t_o)$ must have a non-unique solution for $g'(t)$. This property should be considered in the numerical computation.

The second property of the integral operator $\Lambda(t_o)$ is as follows:

$$I_1 = \int_\Gamma \Lambda(t_o)\,dt_o = 0 \tag{40}$$

In fact, from Eqs. (21) and (34), the left side of Eq. (40) can be rewritten as

$$I_1 = \frac{1}{2\pi}(I_{11} + I_{12}) \tag{41}$$

where

$$I_{11} = \int_\Gamma \left(\int_\Gamma \frac{dt_o}{t-t_o} + \int_\Gamma \frac{d\bar{t}_o}{\bar{t}-\bar{t}_o}\right)g'(t)\,dt,$$

$$I_{12} = -\int_\Gamma \left(\int_\Gamma \frac{d}{dt_o}\left\{\frac{t-t_o}{\bar{t}-\bar{t}_o}\right\}dt_o\right)\overline{g'(t)}\,d\bar{t} \tag{42}$$

Clearly, $\int_\Gamma \frac{dt_o}{t-t_o} = -\pi i$, $\int_\Gamma \frac{d\bar{t}_o}{\bar{t}-\bar{t}_o} = \pi i$ and $\int_\Gamma \frac{d}{dt_o}\left\{\frac{t-t_o}{\bar{t}-\bar{t}_o}\right\}dt_o = 0$, thus, the equality (40) is proved.

Substituting Eq. (33) into Eq. (40) yields

$$\int_\Gamma (\tilde{\sigma}_N(t_o) + i\tilde{\sigma}_{NT}(t_o))\,dt_o = 0 \tag{43}$$

Eq. (43) reveals that the applied traction $\tilde{\sigma}_N(t_o) + i\tilde{\sigma}_{NT}(t_o)$ should be equilibrated in resultant forces.
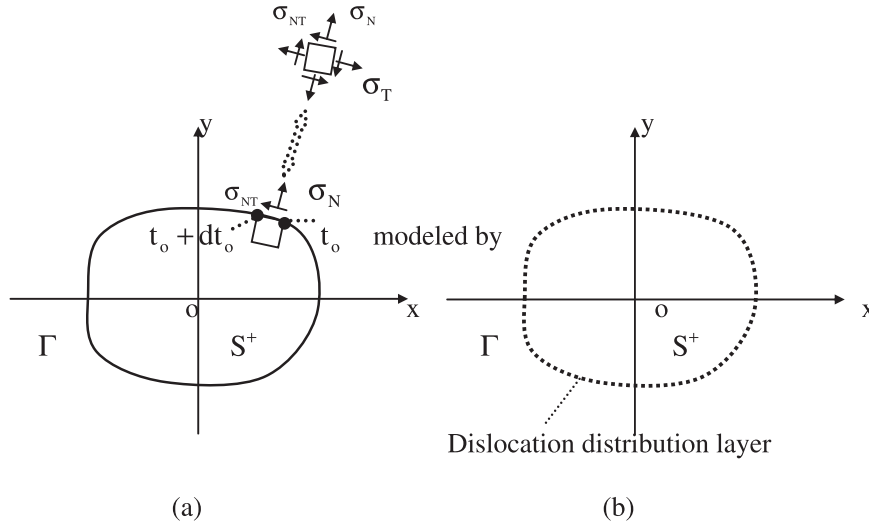
5

Fig. 2. (a) A finite plate with boundary tractions $\sigma_N + i\sigma_{NT}$ in equilibrium. (b) The real problem modeled by the dislocation distribution layer.

The third property of the integral operator $\Lambda(t_o)$ is as follows:

$$I_2 = \text{Re} \int_\Gamma \bar{t}_o \Lambda(t_o)\, dt_o = 0 \tag{44}$$

In fact, from Eqs. (21) and (34), the left side of Eq. (44) can be rewritten as

$$I_2 = \frac{1}{2\pi}(I_{21} + I_{22}) \tag{45}$$

where

$$I_{21} = \text{Re} \int_\Gamma \left(\int_\Gamma \frac{\bar{t}_o\, dt_o}{t - t_o} + \int_\Gamma \frac{\bar{t}_o\, d\bar{t}_o}{\bar{t} - \bar{t}_o} \right) g'(t)\, dt$$

$$= \text{Re} \int_\Gamma \left(\int_\Gamma \frac{\bar{t}_o\, dt_o}{t - t_o} + \int_\Gamma \frac{\bar{t}\, d\bar{t}_o}{\bar{t} - \bar{t}_o} \right) g'(t)\, dt \tag{46}$$

$$I_{22} = \text{Re} \int_\Gamma \left(-\int_\Gamma \bar{t}_o \frac{d}{dt_o}\left\{ \frac{t - t_o}{\bar{t} - \bar{t}_o} \right\} dt_o \right) \overline{g'(t)}\, d\bar{t}$$

$$= \text{Re} \int_\Gamma \left(\int_\Gamma \frac{t - t_o}{\bar{t} - \bar{t}_o}\, d\bar{t}_o \right) \overline{g'(t)}\, d\bar{t}$$

$$= \text{Re} \int_\Gamma \left(\int_\Gamma \frac{\bar{t} - \bar{t}_o}{t - t_o}\, dt_o \right) g'(t)\, dt \tag{47}$$

In Eq. (46), the equality $\int_\Gamma dt_o = \int_\Gamma d\bar{t}_o = 0$ is used. Thus, we have

$$I_{21} + I_{22} = \text{Re} \int_\Gamma \left(\int_\Gamma \frac{\bar{t}\, dt_o}{t - t_o} + \int_\Gamma \frac{\bar{t}\, d\bar{t}_o}{\bar{t} - \bar{t}_o} \right) g'(t)\, dt$$

$$= \text{Re} \int_\Gamma \left(\int_\Gamma \frac{dt_o}{t - t_o} + \int_\Gamma \frac{d\bar{t}_o}{\bar{t} - \bar{t}_o} \right) \bar{t} g'(t)\, dt = 0 \tag{48}$$

Clearly, from the equalities $\int_\Gamma \frac{dt_o}{t - t_o} = -\pi i$, $\int_\Gamma \frac{dt_o}{\bar{t} - \bar{t}_o} = \pi i$, the equality (44) is proved.

Substituting Eq. (33) into Eq. (44) yields

$$\text{Re} \int_\Gamma (\tilde{\sigma}_N(t_o) + i\tilde{\sigma}_{NT}(t_o))\bar{t}_o\, dt_o = 0 \tag{49}$$

Eq. (49) reveals that the applied traction $\tilde{\sigma}_N(t_o) + i\tilde{\sigma}_{NT}(t_o)$ should be equilibrated in moment.

3.3. Numerical solution for the interior BVP and numerical example

Generally, the integral equation shown by Eq. (33) is solved numerically after discretization. The ellipse has two half-axes "a" and "b" (Fig. 3). It is assumed that the stress fields are derived from the following complex potentials:

$$\Phi(z) = Cp, \quad \Psi(z) = Dp \text{ (taking } C = 1 + 0.5i, D = 2 + 1.5i) \tag{50}$$

where "p" is a unit loading, and C and D are two constants. Clearly, the tractions σ_N, σ_{NT}, σ_T applied along the elliptic contour can easily evaluated from the assumed complex potentials. The evaluated
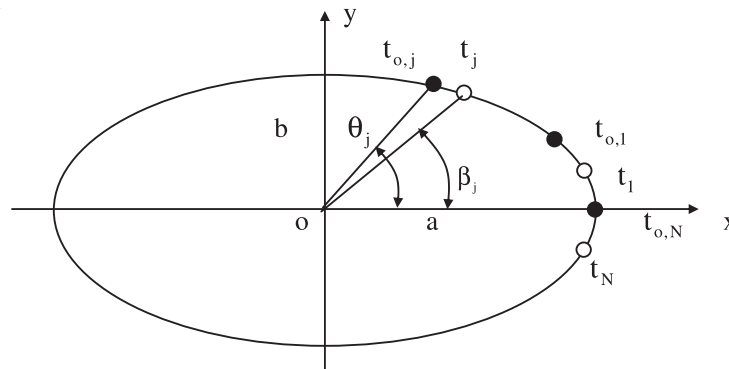

Fig. 3. Nodes assumed along the elliptic boundary.

components σ_N and σ_{NT} become the right hand term in the integral equation (33).

In the discretization for the integral equation, the following quadrature rule is suggested (Zemlyanova, 2007):

$$\int_0^{2\pi} f(\beta)s(\beta,\theta)\,d\beta = \frac{2\pi}{N}\sum_{j=1}^{N} f(\beta_j)s(\beta_j,\theta),$$

$$\beta_j = \frac{(2j-1)\pi}{N} + \delta,$$

$$(\delta - \text{any positive value}, \quad j = 1,2,\ldots,N) \tag{51}$$

In the first case, the kernel $s(\beta,\theta)$ is regular and Eq. (51) can be used to any θ. In the second case, the kernel $s(\beta,\theta)$ is singular, for example, $s(\beta,\theta) = 1/(\beta-\theta)$. In this case, Eq. (51) is valid for the following θ_k:

$$\theta = \theta_k = \frac{2k\pi}{N} + \delta, \quad (k = 1,2,\ldots,N) \tag{52}$$

Once the values for $f(\beta_j)$, $j = 1,2,\ldots,N$ are obtained, the function $f(\theta)$ $(0 < \theta < 2\pi)$ can be obtained from the following interpolation equation (Zemlyanova, 2007):

$$f(\theta) = \frac{1}{N}\sum_{j=1}^{N} f(\beta_j)\sin\frac{N(\beta_j-\theta)}{2}\cot\frac{\beta_j-\theta}{2} \quad (0 < \theta < 2\pi) \tag{53}$$

After using the quadrature rule shown by Eq. (51), the integral equation (33) can be reduced to the following system of algebraic equations:

$$\mathbf{Ax} = \mathbf{p} \tag{54}$$

where $\mathbf{A}$ is a matrix with dimension $2N \times 2N$. In Eq. (54), two vectors $\mathbf{x}$ and $\mathbf{p}$ are defined by

$$\mathbf{x} = \left\{ \text{Reg}'(t_1)\text{Img}'(t_1)\ldots\text{Reg}'(t_j)\text{Img}'(t_j)\ldots\text{Reg}'(t_N)\text{Img}'(t_N) \right\}^T \tag{55}$$

$$\mathbf{p} = \left\{ \sigma_N(t_{o,1})\sigma_{NT}(t_{o,1})\ldots\sigma_N(t_{o,j})\sigma_{NT}(t_{o,j})\ldots\sigma_N(t_{o,N})\sigma_{NT}(t_{o,N})\ldots \right\}^T \tag{56}$$

From two conditions shown by Eqs. (43) and (49) we see that, the right hand term of Eq. (33), or the boundary traction $\tilde{\sigma}_N(t_o) + i\tilde{\sigma}_{NT}(t_o)$ should satisfy three equations (here, one complex variable equation equal two in real variable). Alternatively speaking, the existence of solution for the integral equation (33) is conditional. Thus, after discretization, three columns in the matrix must be a linear combination of other $2N - 3$ columns. Therefore, the rank of formulated matrix is $2N - 3$.

Therefore, we have $\det\mathbf{A} = 0$. However, since there are some digital errors in computation, we have $\det\mathbf{A} \neq 0$ in a real computation even though there may be $\det\mathbf{A} \approx 0$. Therefore, we can propose the following four options to solve the algebraic equations:

(1) First case: The matrix $\mathbf{A}$ is not modified.
(2) Second case: Letting $x_1 = 1$, $x_2 = 0$, $x_3 = 0$ in Eq. (54), and solving the algebraic equations.
(3) Third case: Letting $x_1 = 0$, $x_2 = 1$, $x_3 = 0$ in Eq. (54), and solving the algebraic equations.
(4) Forth case: Letting $x_1 = 0$, $x_2 = 0$, $x_3 = 1$ in Eq. (54), and solving the algebraic equations.

It is known that $\sigma_x + \sigma_y$ is an invariant, or $\sigma_x + \sigma_y = \sigma_N + \sigma_T$. Therefore, from Eq. (1) the stress component σ_T along contour can be evaluated by

$$\sigma_T(t_o) = 4\text{Re}\phi'^+(t_o) - \sigma_N(t_o) \tag{57}$$

where

$$\phi'^+(t_o) = \frac{ig'(t_o)}{2} + \frac{1}{2\pi}\int_\Gamma \frac{g'(t)\,dt}{t-t_o} \tag{58}$$

After solving the algebraic equation (54), the stress component $\sigma_T(t_o)$ can be evaluated from Eqs. (57) and (58).

Finally, the computed tangent stress is expressed as

$$\sigma_T = h(\theta)p, \quad 0 \leqslant (\theta) \leqslant 2\pi \tag{59}$$

In computation, we choose $N = 72$, $a = 1$, $b/a = 0.5$, $\kappa = 1.8$. The exact results for $h(\theta)$ and the computed results under four above-mentioned conditions are listed in Table 1. From tabulated results we see that the deviations for stress σ_T between the exact solution and numerical solutions are very small. Clearly, the input data for σ_N and σ_{NT}, or the right hand term of Eq. (33) or (54), must be in equilibrium for the resultant forces and moment. Therefore, the solution for stresses σ_{ij} must be unique in the region S^+. However, the obtained solutions for the intermediate function $g'(t)$ in four cases may not be the same.

Similarly, for the following complex potentials:

$$\Phi(z) = Cp\frac{z}{a}, \quad \Psi(z) = Dp\frac{z}{a}, \ (\text{taking } C = 1 + 0.5i, D = 2 + 1.5i) \tag{60}$$

where "p" is a unit loading, and C and D are two constants. The exact results for $h(\theta)$ and the computed results under four above-mentioned conditions are listed in Table 2. From tabulated results we see that the deviations for stress σ_T between the exact solution and numerical solutions are also very small.

Table 1
Non-dimensional stress $h(\theta)$ $(\sigma_T(\theta) = h(\theta)p)$ at the boundary point $t(\theta)$ $(0 \leqslant \theta \leqslant 2\pi)$ of an elliptic plate for the case of assumed complex potentials $\Phi(z) = (1 + 0.5i)p$, $\Psi(z) = (2 + 1.5i)p$ (see Fig. 3 and Eq. (59)).

θ (°)	Exact	First case	Second case	Third case	Fourth case
30.0	−0.4623	−0.4624	−0.4645	−0.4632	−0.4613
60.0	−0.3425	−0.3425	−0.3440	−0.3432	−0.3419
90.0	0.0000	−0.0002	−0.0014	−0.0007	0.0004
120.0	0.5058	0.5054	0.5040	0.5047	0.5060
150.0	1.7255	1.7244	1.7223	1.7233	1.7252
180.0	4.0000	3.9974	3.9951	3.9951	3.9962
210.0	−0.4623	−0.4624	−0.4611	−0.4620	−0.4635
240.0	−0.3425	−0.3425	−0.3414	−0.3421	−0.3432
270.0	0.0000	−0.0002	0.0011	0.0004	−0.0007
300.0	0.5058	0.5054	0.5071	0.5063	0.5049
330.0	1.7255	1.7244	1.7277	1.7263	1.7238
360.0	4.0000	3.9974	3.9906	3.9941	3.9985

Table 2
Non-dimensional stress $h(\theta)(\sigma_T(\theta) = h(\theta)p)$ at the boundary point $t(\theta)$ $(0 \leqslant \theta \leqslant 2\pi)$ of an elliptic plate for the case of assumed complex potentials $\Phi(z) = (1 + 0.5i)pz/a$, $\Psi(z) = (2 + 1.5i)pz/a$ (see Fig. 3 and Eq. (59)).

θ (°)	Exact	First case	Second case	Third case	Fourth case
30.0	−1.3843	−1.3846	−1.3858	−1.3846	−1.3826
60.0	−0.5557	−0.5556	−0.5565	−0.5558	−0.5545
90.0	0.0000	0.0002	−0.0006	0.0000	0.0011
120.0	0.2028	0.2031	0.2021	0.2028	0.2041
150.0	−0.7641	−0.7633	−0.7648	−0.7638	−0.7620
180.0	−5.0000	−4.9970	−4.9985	−4.9985	−4.9975
210.0	1.3843	1.3846	1.3855	1.3846	1.3831
240.0	0.5557	0.5556	0.5565	0.5558	0.5546
270.0	0.0000	−0.0002	0.0006	0.0000	−0.0011
300.0	−0.2028	−0.2031	−0.2020	−0.2028	−0.2043
330.0	0.7641	0.7633	0.7652	0.7639	0.7614
360.0	5.0000	4.9970	4.9947	4.9981	5.0026

7

4. Dislocation distribution layer method for the solution of exterior boundary value problem (BVP)

4.1. Formulation of the integral equation for exterior BVP

From Eqs. (25) and (27), we see that the complex potentials shown by Eqs. (18) and (19) can only be used to the exterior BVP where the applied tractions are equilibrated in forces and moment. However, in the exterior BVP, the applied boundary tractions may be arbitrary. Therefore, the complex potentials shown by Eqs. (18) and (19) cannot be directly used to the exterior BVP.

In the exterior BVP, from Eq. (4) the boundary condition may be written as (Fig. 4)

$$\sigma_N(t_o) + i\sigma_{NT}(t_o) = \tilde{\sigma}_N(t_o) + i\tilde{\sigma}_{NT}(t_o) \quad (t_o \in \Gamma) \quad (61)$$

where the boundary traction $\tilde{\sigma}_N(t_o) + i\tilde{\sigma}_{NT}(t_o)$ is given beforehand, which may not be in equilibrium.

In this case, one may assume the complex potentials in the following form:

$$\phi(z) = \phi_1(z) + \phi_2(z) + \phi_3(z),$$
$$\psi(z) = \psi_1(z) + \psi_2(z) + \psi_3(z), \quad (z \in S^-) \quad (62)$$

where

$$\phi_1(z) = -\frac{1}{2\pi} \int_\Gamma \ln(z-t) g'(t) \, dt \quad (492)$$

$$\psi_1(z) = -\frac{1}{2\pi} \int_\Gamma \ln(z-t) \overline{g'(t)} \, d\bar{t} - \frac{1}{2\pi} \int_\Gamma \frac{\bar{t} g'(t) \, dt}{t-z}, \quad (z \in S^-) \quad (63)$$

$$\phi_2(z) = F \ln z, \qquad \psi_2(z) = -\kappa \overline{F} \ln z + \frac{m_o i}{2\pi z}, \quad (z \in S^-) \quad (64)$$

$$\phi_3(z) = \frac{H}{2\pi} \ln z, \qquad \psi_3(z) = \frac{\overline{H}}{2\pi} \ln z \quad (z \in S^-) \quad (65)$$

$$H = H_1 + iH_2, \quad F = -\frac{P_x + iP_y}{2\pi(\kappa+1)} \quad (66)$$

In Eq. (62), the complex potentials $\phi_1(z)$, $\psi_1(z)$ are used for modeling the dislocation distribution layer along the boundary Γ (Fig. 4). The complex potentials $\phi_2(z)$, $\psi_2(z)$ are used for modeling the condition that there are some resultant forces "F" and moment "m_o"

resulted by tractions applied on the boundary Γ (Fig. 4). The complex potentials $\phi_3(z)$, $\psi_3(z)$ represent a concentrated dislocation with intensity H ($H = H_1 + iH_2$) applied at the origin (Fig. 4). It will be seen later that this term is necessary for the balance of the numbers of the algebraic equations and unknowns after discretization of the integral equations.

After substituting Eqs. (62)–(65) into Eq. (4), using condition (61), and letting $z \to t_o^-$, the following integral equation is obtained:

$$\Lambda(t_o) + \Sigma(t_o) = \tilde{\sigma}_N(t_o) + i\tilde{\sigma}_{NT}(t_o) - \big(\tilde{\sigma}_{N(2)}(t_o) + i\tilde{\sigma}_{NT(2)}(t_o)\big), \quad (t_o \in \Gamma) \quad (67)$$

where

$$\Lambda(t_o) = \frac{1}{\pi} \int_\Gamma \frac{g'(t) \, dt}{t-t_o} + \frac{1}{2\pi} \int_\Gamma K_1(t, t_o) g'(t) \, dt$$
$$+ \frac{1}{2\pi} \int_\Gamma K_2(t, t_o) \overline{g'(t)} \, d\bar{t}, \quad (t_o \in \Gamma) \quad (68)$$

$$\Sigma(t_o) = \frac{H}{2\pi} \left(\frac{1}{t_o} + \frac{1}{\bar{t}_o} \frac{d\bar{t}_o}{dt_o} \right) + \frac{\overline{H}}{2\pi} \left(\frac{1}{\bar{t}_o} - \frac{t_o}{\bar{t}_o^2} \frac{d\bar{t}_o}{dt_o} \right), \quad (t_o \in \Gamma) \quad (69)$$

$$\tilde{\sigma}_{N(2)}(t_o) + i\tilde{\sigma}_{NT(2)}(t_o) = F \left(\frac{1}{t_o} - \kappa \frac{1}{\bar{t}_o} \frac{d\bar{t}_o}{dt_o} \right) + \overline{F} \left(\frac{1}{\bar{t}_o} - \frac{t_o}{\bar{t}_o^2} \frac{d\bar{t}_o}{dt_o} \right)$$
$$+ \frac{m_o i}{2\pi \bar{t}_o^2} \frac{d\bar{t}_o}{dt_o}, \quad (t_o \in \Gamma) \quad (70)$$

In Eq. (67), the term $\tilde{\sigma}_{N(2)}(t_o) + i\tilde{\sigma}_{NT(2)}(t_o)$ is derived from the complex potentials $\phi_2(z)$, $\psi_2(z)$ and Eq. (4), which is known beforehand. An integral equation similar to Eq. (67) was obtained previously (Savruk, 1981).

It is seen from the structure of the complex potentials and Eq. (3) that the displacement expression contains the logarithmic function. Therefore, from the complex potentials shown by Eqs. (62)–(65), we will find the singled-valued condition of displacements as follows:

$$\int_\Gamma g'(t) \, dt - H = 0 \quad (71)$$

Finally, in the exterior BVP, the governing equations are composed of Eqs. (67) and (71).

After discretization, the integral equation will be reduced to a system of linear algebraic equations. It is well known that the

● concentrated forces P_x, P_y and moment m_o

○ concentrated dislocation H

(a) (b)
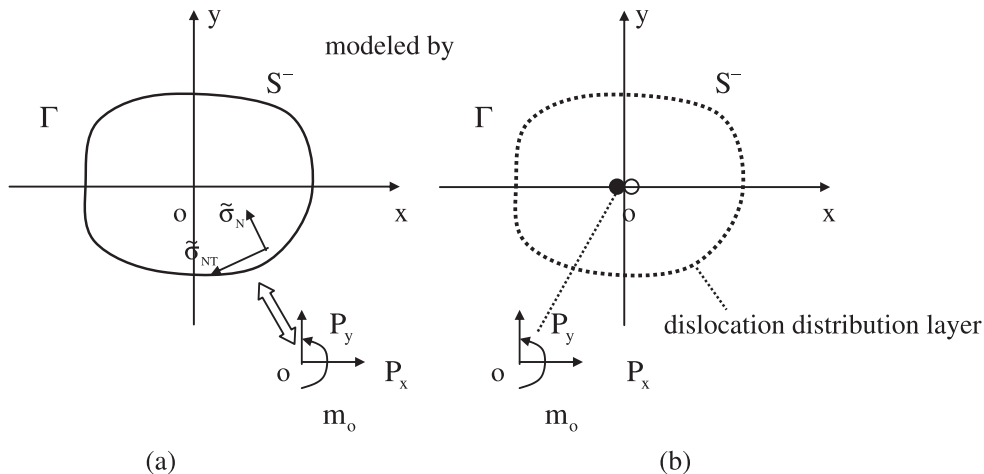
Fig. 4. (a) A notched infinite plate with boundary tractions $\tilde{\sigma}_N + i\tilde{\sigma}_{NT}$ not in equilibrium. (b) The real problem modeled by concentrated forces (P_x, P_y), moment (m_o), dislocation (H) and the dislocation distribution layer.

balance of the numbers of equations and unknowns in the resultant algebraic equation is important. If the balance is not satisfied, the algebraic equation will have no solution, or non-unique solution.

It is assumed that we do not introduce the complex potentials $\phi_3(z)$, $\psi_3(z)$ shown by Eqs. (65) or let H=0. In this case, we will obtain $2N + 2$ equations with $2N$ unknowns in the resultant algebraic equation, if the quadrature rule (51) is used.

In the meantime, after introducing the complex potentials shown by Eq. (65), or introduce the unknown H, we will obtain $2N + 2$ equations with $2N + 2$ unknowns in the resultant algebraic equation, if the quadrature rule (51) is used. This is an advantage for introducing the complex potentials $\phi_3(z)$, $\psi_3(z)$. Clearly, the necessity of the assumed complex potentials $\phi_3(z)$, $\psi_3(z)$ is only from the technical consideration. For the solution of a branch crack problem, a similar idea was proposed in Chen and Hasebe (1995).

The detailed steps in computation are introduced below. After discretization by using the quadrature rule shown by Eqs. (51), from Eq. (67) we will formulate $2N$ algebraic equations at N observation points $t_{o,j}$ at the angles $\theta_j = 2j\pi/N$ $(j = 1, 2, \ldots, N)$, and from Eq. (71) we will formulate two algebraic equations. Therefore, the total algebraic equations are $2N + 2$. In addition, in Eqs. (67) and (71) after discretization by using the quadrature rule shown by Eqs. (51), we will find $2N$ unknowns $(\text{Re}g'(t_k), \text{Im}g'(t_k))$ at N integration points t_k with the angles $\beta_k = (2k - 1)\pi/N$ $(k = 1, 2, \ldots, N)$, and H_1, H_2. Thus, the total unknowns are also $2N + 2$. Thus, the number of the algebraic equations is equal to number of unknowns in the formulation.

4.2. Discussion for the integral equation for exterior BVP

In order to study the behaviors of the integral equation for exterior BVP, we prefer to consider the case that: (1) the tractions applied on contour are in equilibrium in forces and moment, (2) the portion of complex potentials $\phi_3(z)$, $\psi_3(z)$ are deleted. In this case, from Eqs. (67) and (71) we have the following system of the integral equations:

$$\Lambda(t_o) = \tilde{\sigma}_N(t_o) + i\tilde{\sigma}_{NT}(t_o), \quad (t_o \in \Gamma) \tag{72}$$

$$\int_\Gamma g'(t)\,dt = 0 \tag{73}$$

Clearly, Eq. (72) is exactly same as its counterpart equation (33) in the interior BVP.

It is necessary to consider the following two problems. The first is about the conditions for existence of solution for Eq. (72). The second one is if there is a solution from Eq. (72), which satisfies Eq. (73).

Since the structure of Eq. (72) is same as Eq. (33), the conditions for existence of solution for Eq. (72) are still expressed by Eqs. (43) and (49). One may substitute all possible solutions from Eq. (72) into Eq. (73), and find a solution as follows:

$$g'(t) = g_p(t) + c \quad (c - \text{real}) \tag{74}$$

where $g_p(t)$ represents a particular solution.

It was shown by Eqs. (23) and (28) that, the solution $g'(t) = c$ creates the following stress fields: (1) $\phi'(z) = icz$, $\psi'(z) = 0$ (with no stresses anywhere for $z \in S^+$), and (2) $\phi'(z) = 0$, $\psi'(z) = 0$ (with no stresses anywhere for $z \in S^-$). Moreover, the function $g'(t) = c$ also satisfies $\int_\Gamma g'(t)\,dt = 0$ shown by Eq. (73). That is to say, the portion of solution $g'(t) = c$ has no real influence to the stress field. For example, we can obtain the stress component σ_T (in the following numerical example) along the contour.

If one makes discretization to Eqs. (72) and (73), the physical situation of the problem has not been changed. In this case, we can get the correct solution from algebraic equation. However, the correct solution is not coming from the rank improvement in the matrix. On contrary, the correct solution is coming from the facts that, (1) the solution $g'(t) = c$ satisfies the following two equations: (1) $\Lambda(t_o)|_{g'(t)=c} = 0$, $(t_o \in \Gamma)$, (2) $\int_\Gamma g'(t)\,dt = 0$, and (2) $g'(t) = c$ has no influence for the stress field.

4.3. Numerical solution for the exterior BVP and numerical example

Generally, the integral equations shown by Eqs. (67) and (71) are solved numerically after discretization. In the example, the ellipse has two half-axes "a" and "b". It is assumed that the stress fields are derived from the following complex potentials:

$$\Phi(z) = \frac{F}{z - z_g}, \qquad \Psi(z) = -\frac{\kappa\overline{F}}{z - z_g} - \frac{m_g i}{2\pi(z - z_g)^2}, \quad (z \in S^-) \tag{75}$$

where

$$F = -\frac{P_x + iP_y}{2\pi(\kappa + 1)} \tag{76}$$

In Eq. (75), z_g (location of a point), F (or $P_x P_y$, resultant forces), m_g (moment) are given beforehand (Figs. 4 and 5).

Clearly, the tractions σ_N, σ_{NT}, σ_T applied along the elliptic contour can easily be evaluated from the assumed complex potentials. The evaluated components σ_N and σ_{NT} become the term $\tilde{\sigma}_N(t_o) + i\tilde{\sigma}_{NT}(t_o)$ in the right hand term of the integral Eq. (67).

It is seen that the resultant forces from boundary tractions on the contour are P_x and P_y. In addition, from Eqs. (6)–(8), the relevant moment from boundary tractions on the contour is as follows:

$$m_o = m_g + 2\kappa\pi\text{Im}(\overline{F}z_g) \tag{77}$$

Therefore, from the complex potentials shown by Eq. (64) and the given values for P_x, P_y and m_o, the term $\tilde{\sigma}_{N(2)}(t_o) + i\tilde{\sigma}_{NT(2)}(t_o)$ in the right hand term of the integral equation (75) can be evaluated by using Eq. (70).

As in the previous example, the quadrature rule shown by Eq. (51) is used in the discretization of the integral equations. In computation, we assume $N = 72$, $a = 2$ and $b/a = 0.5$. In addition, three loading cases are assumed as follows:

(1) First case: letting $P_x = ap$, $P_y = 0$, $m_g = 0$ in Eqs. (75) and (76).
(2) Second case: letting $P_x = 0$, $P_y = ap$, $m_g = 0$ in Eqs. (75) and (76).
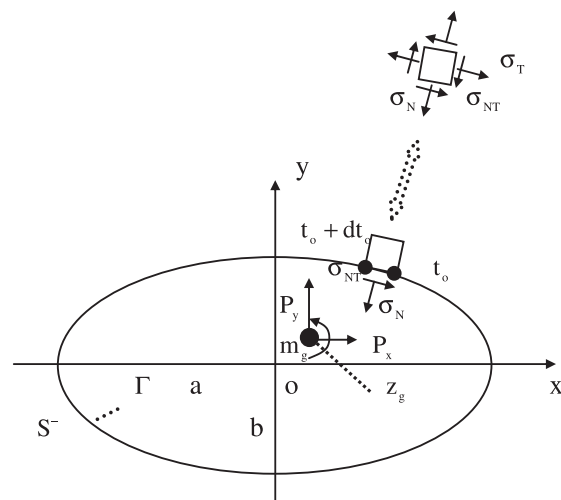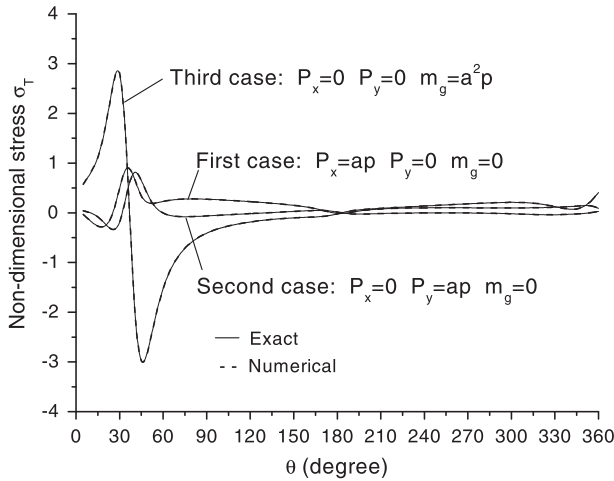(3) Third case: letting $P_x = 0$, $P_y = 0$, $m_g = a^2p$ in Eqs. (75) and (76).

Fig. 5. An exterior BVP with the elliptic boundary.

Fig. 6. Non-dimensional stress $h(\theta)$ $(\sigma_T(\theta) = h(\theta)p)$ at the boundary point $t(\theta)$ $(0 \leqslant \theta \leqslant 2\pi)$ along an elliptic contour for the complex potentials $\Phi(z) = F$ $/(z - z_g)$, $\Psi(z) = -\kappa\overline{F}/(z - z_g) - m_g i/\left(2\pi(z - z_g)^2\right)$ with $b/a = 0.5$, $F = -(P_x + iP_y)/$ $(2\pi(\kappa + 1))$, $z_g = 0.5a + (0.5b)i$, for three cases: (1) $P_x = ap$, $P_y = 0$, $m_g = 0$, (2) $P_x = 0$, $P_y = ap$, $m_g = 0$ (3) $P_x = 0$, $P_y = 0$, $m_g = a^2 p$ (see Fig. 5).

After solving the relevant algebraic equation, the stress component σ_T can be evaluated by

$$\sigma_T(t_o) = 4\mathrm{Re}\Phi^-(t_o) - \sigma_N(t_o) \tag{78}$$

where

$$\Phi^-(t_o) = -\frac{ig'(t_o)}{2} + \frac{1}{2\pi}\int_\Gamma \frac{g'(t)\,dt}{t - t_o} + \frac{F}{t_o} + \frac{H}{2\pi t_o} \tag{79}$$

Finally, the computed tangent stress σ_T is expressed as

$$\sigma_T = h(\theta)p, \quad (0 \leqslant \theta \leqslant 2\pi) \tag{80}$$

Table 3
Non-dimensional stress $h(\theta)(\sigma_T(\theta) = h(\theta)p)$ at the boundary point $t(\theta)$ $(0 \leqslant \theta \leqslant 2\pi)$ along an elliptic contour for the complex potentials $\Phi(z) = F/(z - z_g)$, $\Psi(z) = -\kappa\overline{F}$ $/(z - z_g) - m_g i/\left(2\pi(z - z_g)^2\right)$ with $b/a = 0.5$, $F = -(P_x + iP_y)/(2\pi(\kappa + 1))$, $z_g = 0.5a$ $+(0.5b)i$, for three cases: (1) $P_x = ap$, $P_y = 0$, $m_g = 0$, (2) $P_x = 0$, $P_y = ap$, $m_g = 0$, and (3) $P_x = 0$, $P_y = 0$, $m_g = a^2p$ (see Fig. 5).

θ (°)	First case		Second case		Third case	
	Exact	Numerical	Exact	Numerical	Exact	Numerical
15.0	−0.2833	−0.2872	−0.0761	−0.0685	1.0816	1.0532
30.0	0.5064	0.5211	−0.2854	−0.2923	3.1941	3.2464
45.0	0.2915	0.2803	0.6685	0.6587	−3.2398	−3.2426
60.0	0.2284	0.2319	−0.0154	−0.0081	−1.5013	−1.5110
75.0	0.2776	0.2761	−0.0801	−0.0850	−0.7054	−0.6970
90.0	0.2728	0.2738	−0.0637	−0.0602	−0.4074	−0.4137
105.0	0.2517	0.2512	−0.0396	−0.0422	−0.2650	−0.2599
120.0	0.2244	0.2248	−0.0165	−0.0145	−0.1840	−0.1879
135.0	0.1918	0.1915	0.0056	0.0041	−0.1332	−0.1302
150.0	0.1504	0.1506	0.0279	0.0290	−0.1016	−0.1038
165.0	0.0835	0.0833	0.0479	0.0470	−0.0831	−0.0815
180.0	−0.0159	−0.0157	0.0154	0.0160	−0.0223	−0.0233
195.0	0.0362	0.0360	−0.0260	−0.0263	0.0609	0.0613
210.0	0.0784	0.0786	−0.0161	−0.0160	0.0894	0.0896
225.0	0.0939	0.0937	−0.0066	−0.0064	0.1130	0.1123
240.0	0.0997	0.0999	−0.0016	−0.0020	0.1364	0.1378
255.0	0.1012	0.1010	−0.0005	0.0001	0.1591	0.1570
270.0	0.1006	0.1008	−0.0030	−0.0039	0.1808	0.1834
285.0	0.0992	0.0989	−0.0093	−0.0080	0.1998	0.1959
300.0	0.0983	0.0986	−0.0202	−0.0218	0.2101	0.2150
315.0	0.1013	0.1010	−0.0342	−0.0321	0.1947	0.1887
330.0	0.1113	0.1118	−0.0397	−0.0425	0.1249	0.1329
345.0	0.1326	0.1319	−0.0232	−0.0195	0.0710	0.0599
360.0	0.0909	0.0924	0.0273	0.0221	0.4074	0.4238

The exact results for $h(\theta)$ and the computed results for three above-mentioned cases are plotted in Fig. 6 and listed in Table 3. In Fig. 6, the exact results are plotted with the solid line and the numerical exact results are plotted with the dashed line. Since two results for the function $h(\theta)$ are very close, the two curves are merged into one. From Table 3 we see that at $\theta = 45°$ of third case, $h(\theta)$ takes the value: −3.2398 (from exact solution); −3.2426 (from numerical solution). From the plotted and tabulated results we see that the deviations for stress σ_T between the exact solution and numerical solution are very small.

The second example is devoted to a rectangular contour with the rounded corner under the remote tension $\sigma_x^\infty = \sigma_x^\infty = p$ (Fig. 7). The problem can be reduced to an exterior BVP with the tractions on the contour only. The reduced problem can be solved by using the suggested method.

In computation, we assume $N = 120$, $a = 2$, $b/a = 0.5, 0.6, \ldots, 1.0$, and $c = 0.5b$. Finally, the computed tangent stress σ_T is expressed as
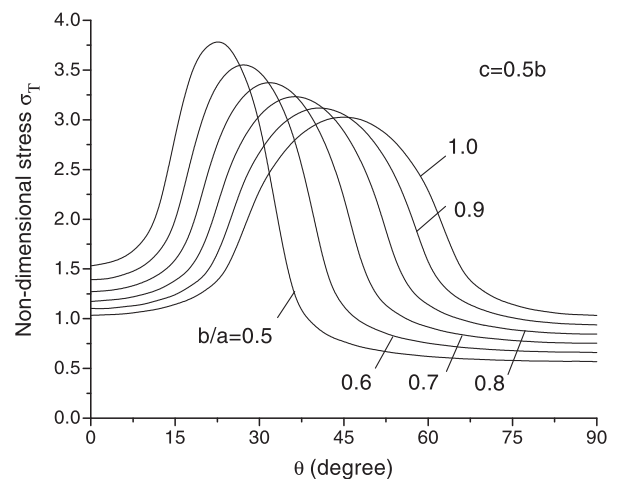
$$\sigma_T = h(b/a, \theta)p, \quad (0 \leqslant \theta \leqslant \pi/2) \tag{81}$$

The computed results for $h(b/a, \theta)$ are plotted in Fig. 8 and listed in Table 4.

From tabulated results in Table 4, we see that a significant stress concentration factor has been found. For example, we have $h(b/a, \theta)_{\max}|_{b/a=0.5, \theta=24°} = 3.805$, $h(b/a, \theta)_{\max}|_{b/a=0.7, \theta=33°} = 3.382$,
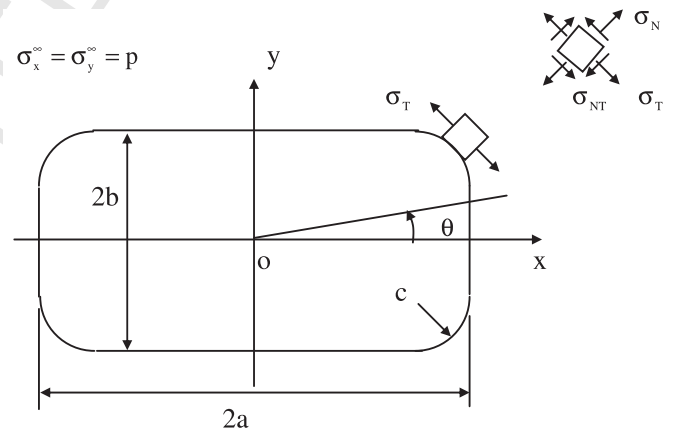
Fig. 7. An exterior BVP for a rectangular contour with the rounded corner.

Fig. 8. Non-dimensional stresses $h(b/a, \theta)$ $(= \sigma_T/p)$ at the boundary point $t(\theta)$ $(0 \leqslant \theta \leqslant \pi/2)$ along a rounded rectangular contour (see Fig. 7).

Table 4

Non-dimensional stresses $h(b/a, \theta)$ $(= \sigma_T/p)$ at the boundary point $t(\theta)$ $(0 \leqslant \theta \leqslant \pi/2)$ along a rounded rectangular contour (see Fig. 7).

θ (°)	$b/a =$					
	0.5	0.6	0.7	0.8	0.9	1.0
0	1.532	1.393	1.271	1.174	1.103	1.033
3	1.557	1.395	1.280	1.186	1.099	1.040
6	1.611	1.444	1.305	1.199	1.122	1.047
9	1.746	1.507	1.354	1.239	1.137	1.071
12	2.011	1.650	1.435	1.285	1.187	1.095
15	2.858	1.915	1.567	1.381	1.232	1.144
18	3.555	2.672	1.857	1.503	1.338	1.199
21	3.779	3.226	2.534	1.835	1.458	1.304
24	3.805	3.486	2.993	2.442	1.841	1.452
27	3.515	3.578	3.244	2.816	2.377	1.868
30	3.032	3.506	3.373	3.057	2.682	2.316
33	2.064	3.268	3.382	3.195	2.911	2.580
36	1.184	2.882	3.282	3.245	3.046	2.795
39	0.964	2.216	3.071	3.212	3.120	2.924
42	0.829	1.383	2.740	3.098	3.122	3.013
45	0.769	1.100	2.253	2.898	3.064	3.032
48	0.711	0.959	1.539	2.605	2.937	3.013
51	0.684	0.882	1.192	2.186	2.738	2.924
54	0.653	0.820	1.066	1.573	2.465	2.795
57	0.638	0.785	0.969	1.257	2.051	2.580
60	0.618	0.750	0.915	1.136	1.520	2.316
63	0.610	0.732	0.868	1.041	1.296	1.868
66	0.597	0.710	0.840	0.989	1.174	1.452
69	0.593	0.700	0.812	0.942	1.101	1.304
72	0.583	0.685	0.796	0.915	1.044	1.199
75	0.581	0.680	0.779	0.888	1.010	1.144
78	0.575	0.670	0.771	0.874	0.980	1.095
81	0.575	0.668	0.761	0.858	0.964	1.071
84	0.570	0.662	0.758	0.853	0.948	1.047
87	0.571	0.663	0.752	0.845	0.943	1.040
90	0.568	0.660	0.753	0.846	0.938	1.033

and $h(b/a, \theta)_{\max}|_{b/a=1.0, \theta=45°} = 3.032$. We know that for the circular hole case, the stress concentration factor is 2 under the remote tension $\sigma_x^\infty = \sigma_x^\infty = p$.

5. Conclusions

Based on a previous publication (Savruk, 1981), this paper studies the formulation and numerical solutions of the interior and exterior boundary value problems in plane elasticity, which is based on the dislocation distribution layer in an infinite plate. In addition, the formulation of dislocation distribution layer mainly relies on the relevant complex potentials, or some complex variable functions.

The complex variable plays an important role in the analysis. For example, a complex potential in Eq. (17) was expressed by $\phi(z) = -(1/2\pi) \int_\Gamma \ln(z - t) g'(t) \, dt$. When a moving point "$z$" moves along a closed loop in the region $z \in S^+$, the term $\ln(z - t)$ is a

single-valued analytic function. Similar situation holds for the complex potential $\psi(z)$ shown by Eq. (18). Therefore, the single-valued condition of displacements is satisfied automatically, if the dislocation distribution method is used for the interior problem.

However, for the same complex potential $\phi(z) = -(1/2\pi) \int_\Gamma \ln(z - t) g'(t) \, dt$, when a moving point "$z$" moves along a closed loop in the region $z \in S^-$, the term $\ln(z - t)$ is a multiple-valued analytic function. Similar situation holds for the complex potential $\psi(z)$ shown by Eq. (18). Therefore, the single-valued condition of displacements must be imposed, if the dislocation distribution method is used for the exterior problem.

Physically, the applied tractions on the boundary must be in equilibrium for the interior problem. However, this property is not easy to prove in the direct BIE formulation, which is based on the Somigliana identity (Brebbia et al., 1984). However, this property has been proved successfully in the dislocation distribution method, which can be referred to Eqs. (40), (43), (44) and (49).

From the computed results, it is proved that the dislocation distribution method can provide sufficient accurate results.

References

Brebbia, C.A., Tells, J.C.F., Wrobel, L.C., 1984. Boundary Element Techniques – Theory and Application in Engineering. Springer, Heidelberg.

Chen, Y.Z., 2007. Integral equation methods for multiple crack problems and relevant topics. Applied Mechanics Review 60, 172–194.

Chen, J.T., Chen, Y.W., 2000. Dual boundary element analysis using complex variable for potential problems with or without a degenerate boundary. Engineering Analysis with Boundary Elements 24, 671–684.

Chen, Y.Z., Cheung, Y.K., 1994. A new boundary integral equation for notch problem of plane elasticity. International Journal of Fracture 66, 91–97.

Chen, Y.Z., Hasebe, N., 1995. New integration scheme for the branch crack problem. Engineering Fracture Mechanics 52, 791–801.

Chen, Y.Z., Lin, X.Y., 2006. Complex potentials and integral equations for curved crack and curved rigid line problems in plane elasticity. Acta Mechanica 182, 211–236.

Cheng, A.H.D., Cheng, D.S., 2005. Heritage and early history of the boundary element method. Engineering Analysis with Boundary Elements 29, 286–302.

Cruse, T.A., 1969. Numerical solutions in three-dimensional elastostatics. International Journal of Solids and Structures 5, 1259–1274.

Denda, M., Kosaka, I., 1997. Dislocation and point-force-based approach to the special Green's function BEM for elliptic hole and crack problems in two dimensions. International Journal for Numerical Methods in Engineering 40, 2857–2889.

Jaswon, M.A., Symm, G.T., 1997. Integral Equation Methods in Potential Theory and Elastostatics. Academic Press, London.

Muskhelishvili, N.I., 1953. Some Basic Problems of Mathematical Theory of Elasticity. Noordhoff, Groningen.

Rizzo, F.J., 1967. An integral equation approach to boundary value problems in classical elastostatics. Quarterly Journal of Applied Mathematics 25, 83–95.

Savruk, M.P., 1981. Two-Dimensional Problems of Elasticity for Body with Crack. Naukoya Dumka, Kiev (in Russian).

Whitley, R.J., Hromadka II, T.V., 2006. Theoretical developments in the complex variable boundary element method. Engineering Analysis with Boundary Elements 30, 1020–1024.

Zemlyanova, A., 2007. Singular integral equations for a patch repair problem. International Journal of Solids and Structures 44, 6860–6877.